Thermal conductivity measurement of individual Bi_2Se_3 nano-ribbon by self-heating three-ω method

Guodong Li, Dong Liang, Richard L. J. Qiu, and Xuan P. A. Gao[a)]
Department of Physics, Case Western Reserve University, Cleveland, Ohio 44106, USA

(Received 24 October 2012; accepted 11 January 2013; published online 28 January 2013)

We report thermal conductivity measurements of individual single crystalline Bi_2Se_3 nano-ribbon (NR) synthesized via the gold nanoparticle catalyzed vapor-liquid-solid mechanism. By using the four-probe third harmonic method, thermal conductivity of Bi_2Se_3 NRs was obtained in the temperature range of 10 K to 300 K. It is found that the measured thermal conductivities are nearly two orders of magnitude smaller than the bulk value and have a maximum thermal conductivity at temperature (around 200 K) greater than the bulk. The significant reduced thermal conductivity of NRs is attributed to enhanced phonon boundary scattering in nanostructured material. © *2013 American Institute of Physics*. [http://dx.doi.org/10.1063/1.4789530]

Since Bi_2Se_3 has been shown[1,2] to be a three-dimensional topological insulator possessing robust and nontrivial surface states, much work has been devoted to characterize its 2-dimensional electronic transport properties.[3–6] In the meanwhile, Bi_2Se_3 and some other chalcogenides, such as Bi_2Te_3, Sb_2Te_3 or their alloys also serve as promising thermoelectric (TE) materials for converting waste heat into electrical power or refrigeration.[7–10] Usually, the efficiency of thermoelectric materials is characterized by the dimensionless figure of merit $ZT = S^2\sigma T/\kappa$, where S, σ, κ, and T are the Seebeck coefficient, electrical conductivity, thermal conductivity, and the absolute temperature, respectively. To obtain an efficiency comparable to a household refrigerator for more widespread applications, a ZT value larger than 3 is desired.[11,12] However, for nearly four decades since 1960s, only small progresses have been made on ZT with a practical ceiling of $ZT \approx 1$ for simple crystalline bulk crystal owing to the interdependence of electrical/thermal transport properties and the thermopower.[12]

Recently, several routes have been adopted to enhance the ZT including investigating novel phonon glass electron crystal materials,[13] the effects of doping,[14] and using nanostructured materials,[8,9,15] etc. One central idea in these efforts is to reduce the lattice thermal conductivity without decreasing much of the power factor ($S^2\sigma$). Nanoengineering of thermoelectric materials has been shown to be an effective way to enhance the ZT thanks to strong phonon boundary scatterings in nanostructures. Thermal conductivity measurements on nanowires of Bi_xTe_{1-x}, Si, and SnO_2 indeed revealed that nanowires have thermal conductivity much smaller than the bulk.[16–18] For Bi_2Se_3, Lin *et al.*[19] studied the thermopower of Bi_2Se_3 nanoplates obtained from the decomposition of single-source precursor and reported an enhanced Seebeck coefficient compared to the bulk value. Kadel *et al.*[20] measured the TE properties of solvothermal synthesized Bi_2Se_3 nanostructure and reached a significant reduction in the thermal conductivity owing to the increased boundary scattering for the phonons. However, the TE properties obtained in these two works are ensemble averaging of many nanostructures and till now little is known about the intrinsic TE features of individual Bi_2Se_3 nanowire or nanoribbon (NR). In this work, we synthesized single crystalline Bi_2Se_3 NR by using the Au-catalyed vapor-liquid-solid (VLS) method.[3,6] The thermal conductivity of individual Bi_2Se_3 NR was then measured via the four-point three-ω method.[21] The obtained values of thermal conductivity at the whole measured temperature range are one or two orders of magnitude smaller than the bulk.

The synthesis of single crystalline Bi_2Se_3 NR via VLS method is described elsewhere[6] in a way similar to the VLS growth of other semiconductor NWs.[22–24] The as-grown Bi_2Se_3 NRs had thickness ranging from 50 nm to 400 nm and width ranging from 200 nm to several μms. Energy-dispersive X-ray spectroscopy (EDX) analysis and high-resolution transmission electron microscopy (TEM) imaging show the right stoichiometric Bi_2Se_3 and single-crystalline rhombohedral structure, respectively. For device fabrication, the as grown Bi_2Se_3 NRs on silicon wafer were first dispersed into ethanol solution by sonication and then transferred onto the heavily doped Si substrate with 600 nm thick SiO_2 on surface. Photolithography was used to define the four electrodes pattern. After thermal evaporation of 5-nm-thick Chromium and 150-nm-thick Nickel and a lift-off process, devices each containing a single NR were fabricated. Ohmic contacts were obtained without annealing. To make the NR suspended, which is necessary for performing the thermal conductivity measurement, the fabricated devices were dipped into buffered hydrogen fluoric (HF) acid solution to etch the SiO_2 underneath NR for 1 min. About 100-nm-thick SiO_2 beneath the NR was etched and the Bi_2Se_3 NR was fully suspended, as shown by the scanning electron microscopy (SEM) picture of a typical suspended NR in Fig. 1(a). Note that we noticed that the HF also had etching effect on the metal covering NR and sometimes caused metal layer on top of NR peeling off completely (see S1 in the supplementary material[25]). Nevertheless, many devices maintained the good Ohmic contact after the HF etching process.

The electrical and thermal transport measurements were taken in quantum design physical properties measurement

[a)]Author to whom correspondence should be addressed. Electronic mail: xuan.gao@case.edu.

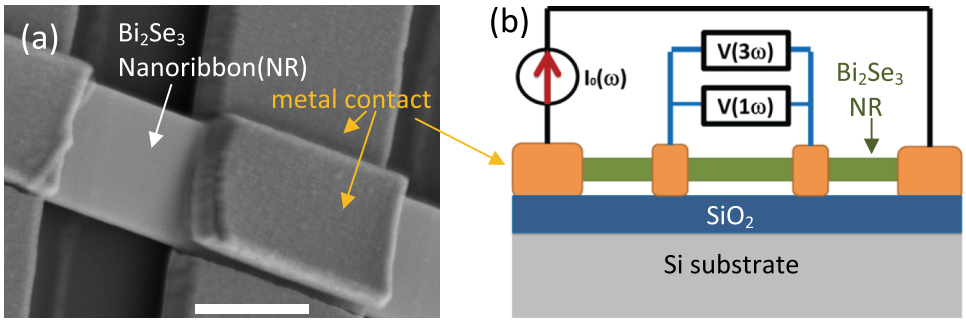

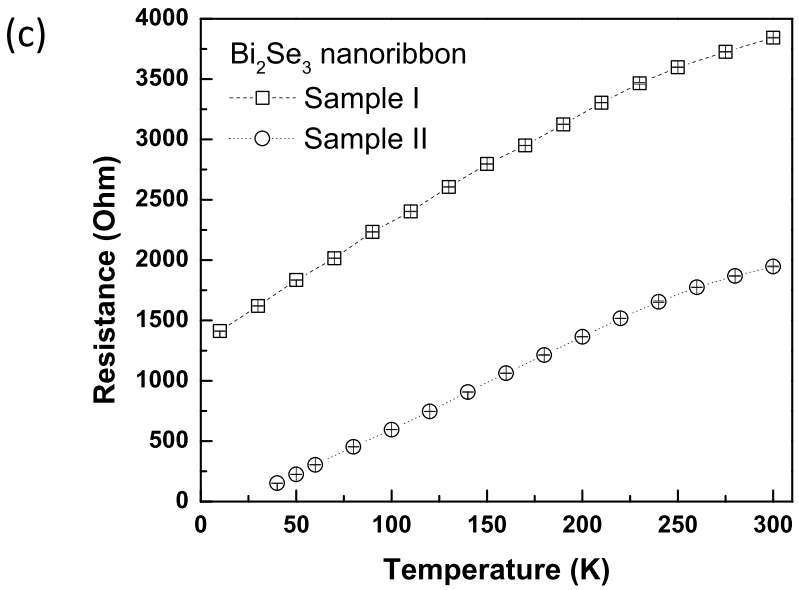

FIG. 1. (a) SEM image of a suspended Bi_2Se_3 nanoribbon device for thermal conductivity measurement. Scale bar is 1.2 μm. (b) A schematic setup of four-probe three-ω method for the thermal conductivity measurement. (c) The resistance as a function of temperature of two Bi_2Se_3 NR devices.

system (PPMS), which was able to provide a control of the bath temperature from 1.9 K to 300 K and a high vacuum (1×10^{-6} Torr) environment, minimizing the gas convection induced heat loss. The radiation heat loss from the surface of nanoribbons is also negligible for the parameters relevant to our experiment (see S2 in the supplementary material[25]). Two lock-in amplifiers (SR830 and LI5640) and one voltage amplifier were used to perform simultaneous electrical and thermal transport measurements. Fig. 1(b) shows the schematic measurement configuration. For the resistance measurement, we used standard four-terminal method by flowing a small AC current I (typically 100 nA to ensure thermal equilibrium with substrate) through the two outer contacts and monitoring the voltage drop V between the two inner contacts. For the thermal conductivity measurement, we used the self-heating 3-ω method, which relies on the suspended conductive NW or NR serving both as a heater and a thermometer.[21,26–28] Specifically, if we apply an AC current $I_0\sin(\omega t)$ to the sample, it creates a temperature fluctuation at frequency of 2ω, which further induces a third harmonic voltage $V_{3\omega}$ across the voltage contacts if the sample resistance varies with temperature. In the limit of $\omega\gamma \rightarrow 0$, where γ is the thermal time constant of the NW or NR, $V_{3\omega}$ can be expressed as[21]

$$V_{3\omega} = \frac{4I_0^3 RR'L}{\pi^4 \kappa S}, \quad (1)$$

where R and R' are the resistance and the derivative of resistance with respect to temperature, respectively, L is the length of the NW or NR between the two voltage probes, S is its cross section, and κ is the thermal conductivity of NW or NR. By fitting the $V_{3\omega}$ signal to cubic dependence of I_0, the thermal conductivity κ can be obtained.

Fig. 1(c) shows temperature dependent resistance of two Bi_2Se_3 NR devices. Sample I had width $w = 1$ μm and thickness $t = 75$ nm and sample II had $w = 500$ nm and $t = 100$ nm as determined by the atomic force microscopy (AFM). The resistance of Bi_2Se_3 NRs generally shows a metallic behavior, which indicates the as grown Bi_2Se_3 NRs were heavily doped presumably due to Se vacancies. The quasi-linear temperature dependence of R suggests electron-phonon scattering as the origin of T-dependent R. From the $R(T)$ curve in Fig. 1(c), the first derivative of resistance can be determined. In the range of temperature (typically $T = 10$-300 K) that the $R(T)$ curve has an appreciable slope, we characterized the temperature dependence of thermal conductivity by the 3ω method. In the 3ω method of thermal conductivity measurement, it is essential to ensure that the measured $V_{3\omega}$ signal is truly generated by the NR, because there could be some spurious 3ω signals related to the current source or contact problem.[27] One consistency check we did in this experiment is to measure the current dependence of resistance due to the Joule heating, which gives a suitable current range to drive the device and an estimate of the 3ω signals from the self-heating of NR. Usually, the cubic-power law dependence of $V_{3\omega}$ on current can be satisfied. The typical current I_0 in 3ω measurement of κ was in the range of several hundreds of nA to several tens of μA depending on sample resistance

(corresponding to an overheating of sample by 1-2 K at the center of suspended NR).

To further validate the extraction of thermal conductivity by 3ω method in our experiment, we study how the 3ω signal varies with input current amplitude I_0 and frequency. Fig. 2(a) presents $V_{3\omega}$ vs. I_0 for sample I at several temperatures and one can see that $V_{3\omega}(I_0)$ follows the I_0^3 dependence well, in agreement with Eq. (1). Thermal conductivity κ is extracted from fitting such $V_{3\omega}$ vs. I_0 data to Eq. (1) with κ as the only fitting parameter. Moreover, it is known that Eq. (1) is only accurate in the limit of $\omega\gamma \to 0$, where the thermal time constant $\gamma = \frac{L^2 C_P \rho}{\pi^2 \kappa}$ in which L is the length of suspended NR between the two voltage probes, C_P is the specific heat, ρ is the mass density. At low frequency, the phase $\phi_{3\omega}$ of measured 3ω signal $V_{3\omega}$ is related to γ as $\tan\phi_{3\omega} \approx 2\omega\gamma$.[21] By fitting $\tan\phi_{3\omega}$ to the frequency $f = \omega/2\pi$ of applied AC current, we estimate the thermal time constant γ in the whole range of temperature being in the order of 10^{-5} s. An example of $\tan\phi_{3\omega}$ vs. f is shown as Fig. 2(b) for sample I at 10 K which shows a linear dependence. Note that we always used frequency lower than 1 KHz when we took the $V_{3\omega}$ vs. I_0 data for the extraction of κ. Thus $\omega\gamma \to 0$ is satisfied during the whole measurement process. The validity of 3ω method for the thermal conductivity of nanowires/nanoribbons is further confirmed in a control measurement on silver nanowires in which very stable 3ω voltage signal was observed and a measured thermal conductivity of 477 W/Km was obtained at 300 K, very close to the bulk value (see S3 in the supplementary material[25]).

The main results of the paper are presented in Fig. 3 which shows the temperature dependence of thermal conductivity of two Bi_2Se_3 NR devices (Fig. 3(a)) and a simple theoretical calculation based on Callaway model[29] (Fig. 3(b)) to compare with experimental data. Two main features stand out in the thermal conductivity data of Bi_2Se_3 NRs. First, in the whole measured temperature range from 30 K to 300 K, the obtained κ ranges from 0.02 W/Km to 0.3 W/Km, which are one or two orders of magnitudes smaller than the bulk values. Second, for both Bi_2Se_3 NR devices, κ vs. T peaks around 200 K, a much higher temperature than the characteristic temperature (~10 K) in the κ vs. T of bulk crystalline Bi_2Se_3.[30] These observations resemble the situation in Bi_2Te_3 NW.[16] Previously, it has been well understood that phonon boundary scattering can greatly suppress the thermal conductivity in nanowires.[16,17] Following the literature,[18,29,30] we consider the frequency-dependent relaxation time of

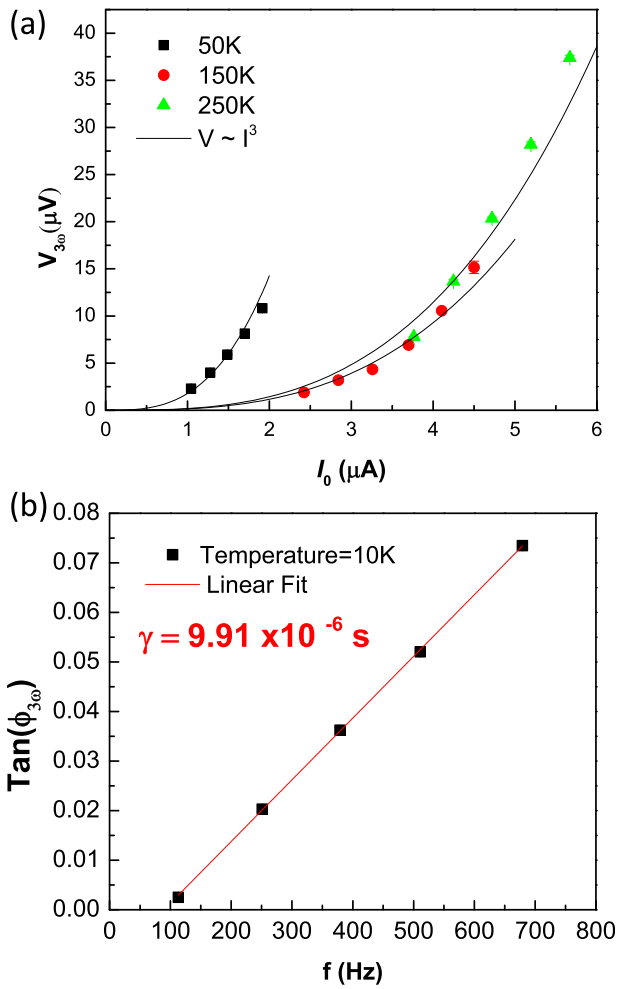

FIG. 2. (a) The third harmonic voltage signal $V_{3\omega}$ as functions of the excitation current amplitude I_0 for sample I at 50, 150 and 250 K. Solid lines show the cubic relationship of $V_{3\omega}$ and I_0. (b) The linear dependence of the tangent of 3-ω signal's phase vs. excitation frequency.

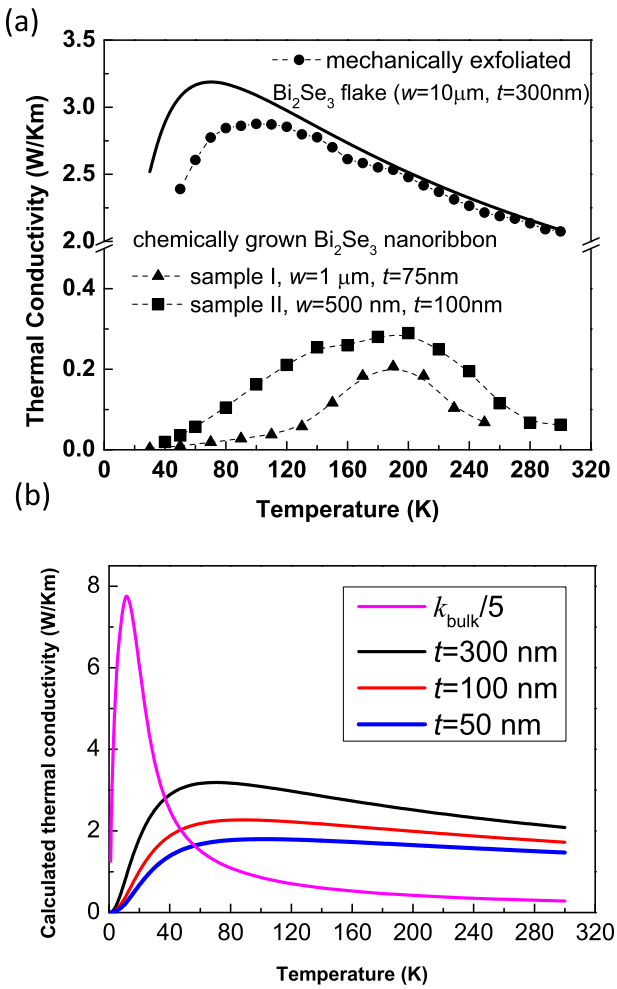

FIG. 3. (a) Thermal conductivity of two Bi_2Se_3 NR devices in the temperature range from 30 K to 300 K together with the measured thermal conductivity of a suspended Bi_2Se_3 flake obtained by mechanical exfoliation. (b) Calculated thermal conductivity for nanostructured Bi_2Se_3 in the Callaway model for different phonon-boundary scattering length t, compared with the bulk thermal conductivity κ_{bulk} of Bi_2Se_3. (κ_{bulk} is reduced by a factor of five to fit into the appropriate scale).

phonons as $\tau^{-1} = \tau_b^{-1} + A\omega^4 + B\omega^2 Texp(-\frac{\theta}{CT})$, where $A\omega^4$ and $B\omega^2 Texp(-\frac{\theta}{CT})$ denote the point-impurity scattering and phonon-phonon Umklapp scattering with parameter A, B, and C being fitted to the bulk value.[29] In the expression of phonon boundary scattering rate, we use $\tau_b^{-1} = v/t$, where v is the phonon velocity of Bi_2Se_3 and t is the critical size of sample (thickness in NRs). Using this simple Callaway model to take into account the boundary scattering, we find that κ is indeed suppressed and the peak temperature moves to higher value than bulk, as shown in Fig. 3(b) for $t = 300$, 100, and 50 nm. However, we fail to achieve a quantitative agreement between the simple Callaway model and data on Bi_2Se_3 NR: the experimental values are still about one order of magnitude smaller than calculation ($\sim$2 K/Wm or smaller) and the temperature of the $\kappa(T)$ peak is only $\sim$100 K for $t = 50$ nm, lower than the $\sim$200 K observed in experiment. Interestingly, as a comparison experiment, we measured the thermal conductivity of a Bi_2Se_3 flake with $w = 10\,\mu$m and $t = 300$ nm obtained by mechanical exfoliation (instead of buffered HF etching of SiO_2 on substrate, the suspension of wide Bi_2Se_3 flake was obtained by pressing cleaved Bi_2Se_3 on scotch tape against prefabricated electrodes on Si/SiO_2 chip). The obtained $\kappa(T)$ data are included in Fig. 3(a) as filled dots and are in reasonable agreement with the Callaway mode for $t = 300$ nm (black solid line). This difference between the thermal conductivity of chemically grown nanoribbons and micro-flakes exfoliated from bulk crystals remains to be further understood.

In summary, we reported the thermal conductivity of individual Bi_2Se_3 NR by using the self-heating 3ω method. In the measured range of temperature (from 10 K to 300 K), the obtained thermal conductivities are one to two orders magnitude smaller than the bulk values. The enhanced phonon boundary scattering can partially explain the reduced the thermal conductivity.

G.D.L. thanks CheeHuei Lee for assistance with the SEM imaging of device. X.P.A.G acknowledges the NSF CAREER Award program (DMR-1151534) and the donors of the American Chemical Society Petroleum Research Fund (Grant No. 48800-DNI10) for support of this research.

[1]H. Zhang, C.-X. Liu, X.-L. Qi, X. Dai, Z. Fang, and S.-C. Zhang, Nature Phys. **5**(6), 438–442 (2009).
[2]Y. Xia, D. Qian, D. Hsieh, L. Wray, A. Pal, H. Lin, A. Bansil, D. Grauer, Y. Hor, and R. Cava, Nature Phys. **5**(6), 398–402 (2009).
[3]H. Peng, K. Lai, D. Kong, S. Meister, Y. Chen, X. L. Qi, S. C. Zhang, Z. X. Shen, and Y. Cui, Nature Mater. **9**(3), 225–229 (2009).
[4]J. Chen, H. Qin, F. Yang, J. Liu, T. Guan, F. Qu, G. Zhang, J. Shi, X. Xie, and C. Yang, Phys. Rev. Lett. **105**(17), 176602 (2010).
[5]J. Checkelsky, Y. Hor, R. Cava, and N. Ong, Phys. Rev. Lett. **106**(19), 196801 (2011).
[6]H. Tang, D. Liang, R. L. J. Qiu and X. P. A. Gao, ACS Nano **5**(9), 7510–7516 (2011).
[7]S. Mishra, S. Satpathy, and O. Jepsen, J. Phys.: Condens. Matter **9**, 461 (1997).
[8]R. Venkatasubramanian, E. Siivola, T. Colpitts, and B. O'quinn, Nature **413**, 597(2001).
[9]B. C. Sales, Science **295**(5558), 1248 (2002).
[10]A. Al Bayaz, A. Giani, A. Foucaran, F. Pascal-Delannoy, and A. Boyer, Thin Solid Films **441**(1), 1–5 (2003).
[11]F. J. DiSalvo, Science **285**(5428), 703–706 (1999).
[12]J. R. Szczech, J. M. Higgins, and S. Jin, J. Mater. Chem. **21**, 4037–4055 (2011).
[13]A. Saramat, G. Svensson, A. Palmqvist, C. Stiewe, E. Mueller, D. Platzek, S. Williams, D. Rowe, J. Bryan, and G. Stucky, J. Appl. Phys. **99**, 023708 (2006).
[14]M. Dresselhaus, G. Chen, Z. Ren, G. Dresselhaus, A. Henry and J. P. Fleurial, JOM **61**(4), 86–90 (2009).
[15]L. D. Hicks and M. S. Dresselhaus, Phys. Rev. B **47**(19), 12727–12731 (1993).
[16]J. Zhou, C. Jin, J. H. Seol, X. Li, and L. Shi, Appl. Phys. Lett. **87**, 133109 (2005).
[17]D. Li, Y. Wu, P. Kim, L. Shi, P. Yang, and A. Majumdar, Appl. Phys. Lett. **83**, 2934 (2003).
[18]L. Shi, Q. Hao, C. Yu, N. Mingo, X. Kong, and Z. L. Wang, Appl. Phys. Lett. **84**, 2638 (2004).
[19]Y. F. Lin, H. W. Chang, S. Y. Lu, and C. Liu, J. Phys. Chem. C **111**(50), 18538–18544 (2007).
[20]K. Kadel, L. Kumari, W. Li, J. Y. Huang, and P. P. Provencio, Nanoscale Res. Lett. **6**, 57 (2011).
[21]L. Lu, W. Yi, and D. L. Zhang, Rev. Sci. Instrum. **72**(7), 2996 (2001).
[22]M. Sakr and X. Gao, Appl. Phys. Lett. **93**(20), 203503 (2008).
[23]D. Liang, M. R. Sakr, and X. P. A. Gao, Nano Lett. **9**(4), 1709–1712 (2009).
[24]P. A. Lin, D. Liang, S. Reeves, X. P. A. Gao, and R. M. Sankaran, Nano Lett. **12**(1), 315–320 (2012).
[25]See supplementary material at http://dx.doi.org/10.1063/1.4789530 for S1: additional SEM image of HF etched Bi_2Se_3 NR device. S2: error estimate of heat loss due to radiation. S3: control experiment on the thermal conductivity of silver nanowire.
[26]T. Y. Choi, D. Poulikakos, J. Tharian, and U. Sennhauser, Appl. Phys. Lett. **87**(1), 013108 (2005).
[27]T. Y. Choi, D. Poulikakos, J. Tharian, and U. Sennhauser, Nano Lett. **6**(8), 1589–1593 (2006).
[28]S. Dhara, H. S. Solanki, R. A. Pawan, V. Singh, S. Sengupta, B. A. Chalke, A. Dhar, M. Gokhale, A. Bhattacharya, and M. M. Deshmukh, Phys. Rev. B **84**(12), 121307(R) (2011).
[29]J. Callaway, Phys. Rev. **113**(4), 1046–1051 (1959).
[30]J. Navratil, J. Horák, T. Plecháček, S. Kamba, P. Lošt'ák, J. Dyck, W. Chen, and C. Uher, J. Solid State Chem. **177**(4), 1704–1712 (2004).